

Overview of Advanced Spaceborne Thermal Emission and Reflection Radiometer (ASTER)

Yasushi Yamaguchi, Anne B. Kahle, Hiroji Tsu, Toru Kawakami, and Moshe Pniel

Abstract—The Advanced Spaceborne Thermal Emission and Reflection Radiometer (ASTER) is a research facility instrument provided by the Ministry of International Trade and Industry (MITI), Tokyo, Japan to be launched on NASA's Earth Observing System morning (EOS-AM1) platform in 1998. ASTER has three spectral bands in the visible near-infrared (VNIR), six bands in the shortwave infrared (SWIR), and five bands in the thermal infrared (TIR) regions, with 15-, 30-, and 90-m ground resolution, respectively. The VNIR subsystem has one backward-viewing band for stereoscopic observation in the along-track direction. Because the data will have wide spectral coverage and relatively high spatial resolution, we will be able to discriminate a variety of surface materials and reduce problems in some lower resolution data resulting from mixed pixels. ASTER will, for the first time, provide high-spatial resolution multispectral thermal infrared data from orbit and the highest spatial resolution surface spectral reflectance temperature and emissivity data of all of the EOS-AM1 instruments.

The primary science objective of the ASTER mission is to improve understanding of the local- and regional-scale processes occurring on or near the earth's surface and lower atmosphere, including surface-atmosphere interactions. Specific areas of the science investigation include the following:

- 1) land surface climatology;
- 2) vegetation and ecosystem dynamics;
- 3) volcano monitoring;
- 4) hazard monitoring;
- 5) aerosols and clouds;
- 6) carbon cycling in the marine ecosystem;
- 7) hydrology;
- 8) geology and soil; and
- 9) land surface and land cover change.

There are three categories of ASTER data: a global map, regional monitoring data sets, and local data sets to be obtained for requests from individual investigators. The ASTER instrument will have a limited (8%) duty cycle. Prioritization of data acquisition requests will be based on such factors as data category, user category, and science discipline.

Index Terms—Advanced Spaceborne Thermal Emission and Reflection Radiometer (ASTER), Earth Observing System (EOS), remote sensing.

Manuscript received October 27, 1997; revised February 3, 1998. This work was supported by the Jet Propulsion Laboratory, California Institute of Technology, under contract with the National Aeronautics and Space Administration (NASA).

Y. Yamaguchi is with the Department of Earth and Planetary Sciences, Nagoya University, Chikusa-ku, Nagoya, 464-01 Japan.

A. B. Kahle and M. Pniel are with the Jet Propulsion Laboratory, California Institute of Technology, Pasadena, CA 91109 USA (anne@lithos.jpl.nasa.gov).

H. Tsu and T. Kawakami are with the Earth Remote Sensing Data Analysis Center, Chuo-ku, Tokyo, 104 Japan.

Publisher Item Identifier S 0196-2892(98)04164-3.

I. INTRODUCTION

THE ADVANCED Spaceborne Thermal Emission and Reflection Radiometer (ASTER) is a research facility instrument provided by the Ministry of International Trade and Industry (MITI), Tokyo, Japan to be launched on NASA's Earth Observing System morning (EOS-AM1) platform in 1998. The primary science objective of the ASTER mission is to improve understanding of the local- and regional-scale processes occurring on or near the earth's surface and lower atmosphere, including surface-atmosphere interactions [1]–[3].

In Japan, the ASTER Instrument Project, the ASTER Ground Data System (GDS), and the ASTER Science Project work together to implement the ASTER mission. A joint Japan/United States science team represents the science community at large to advise the ASTER Instrument Project on requirements and design of the instrument, guides the GDS on instrument operations, and produces algorithms and software for ASTER data products. The ASTER Science Team will support postlaunch operations to ensure that the maximum amount of useful data is acquired by the instrument during its six-year mission.

II. INSTRUMENT DESIGN

A. Overview

Table I shows the baseline performance requirements for the ASTER instrument. The instrument has three separate optical subsystems: the visible and near-infrared (VNIR) radiometer, shortwave-infrared (SWIR) radiometer, and thermal infrared (TIR) radiometer, as shown in Fig. 1. Table II summarizes the characteristic functions of the ASTER subsystems [4]. There are three spectral bands in the VNIR, six bands in the SWIR, and five bands in the TIR regions, with 15-, 30-, and 90-m ground resolution, respectively. Because the data will have wide spectral coverage and relatively high spatial resolution, we will be able to discriminate a variety of surface materials and to reduce problems in some lower spatial resolution data resulting from mixed pixels.

B. Spectral Bandpass

The three VNIR bands have bandpasses similar to those of the Landsat Thematic Mapper (TM) and the Optical Sensor (OPS) of the Japanese Earth Resources Satellite (JERS-1). The VNIR will be especially useful for topographic interpretation because it has along-track stereo coverage in band 3, with nadir (band 3N) and backward (band 3B) views with 15-m

TABLE I
ASTER BASELINE PERFORMANCE REQUIREMENTS

Subsystem	Band No.	Spectral Range (μm)	Radiometric Resolution	Absolute Accuracy (σ)	Spatial Resolution	Signal Quantization Levels
VNIR	1	0.52 - 0.60	$\text{NE}\Delta\rho \leq 0.5\%$	$\leq \pm 4\%$	15 m	8 bits
	2	0.63 - 0.69				
	3N	0.78 - 0.86				
	3B	0.78 - 0.86				
SWIR	4	1.600 - 1.700	$\text{NE}\Delta\rho \leq 0.5\%$	$\leq \pm 4\%$	30 m	8 bits
	5	2.145 - 2.185	$\text{NE}\Delta\rho \leq 1.3\%$			
	6	2.185 - 2.225	$\text{NE}\Delta\rho \leq 1.3\%$			
	7	2.235 - 2.285	$\text{NE}\Delta\rho \leq 1.3\%$			
	8	2.295 - 2.365	$\text{NE}\Delta\rho \leq 1.0\%$			
TIR	9	2.360 - 2.430	$\text{NE}\Delta\rho \leq 1.3\%$	$\leq 3\text{K}(200\text{-}240\text{K})$ $\leq 2\text{K}(240\text{-}270\text{K})$ $\leq 1\text{K}(270\text{-}340\text{K})$ $\leq 2\text{K}(340\text{-}370\text{K})$	90 m	12 bits
	10	8.125 - 8.475	$\text{NE}\Delta T \leq 0.3\text{ K}$			
	11	8.475 - 8.825				
	12	8.925 - 9.275				
	13	10.25 - 10.95				
	14	10.95 - 11.65				
Stereo Base-to-Height Ratio				0.6 (along-track)		
Swath Width				60 km		
Total Coverage in Cross-Track Direction by Pointing				232 km		
MTF at Nyquist Frequency				0.25 (cross-track) 0.20 (along-track)		
Band-to-Band Registration				0.2 pixels (intra-telescope) 0.3 pixels (inter-telescope)		
Peak Data Rate				89.2 Mbps		
Mass				406 kg		
Peak Power				726 W		

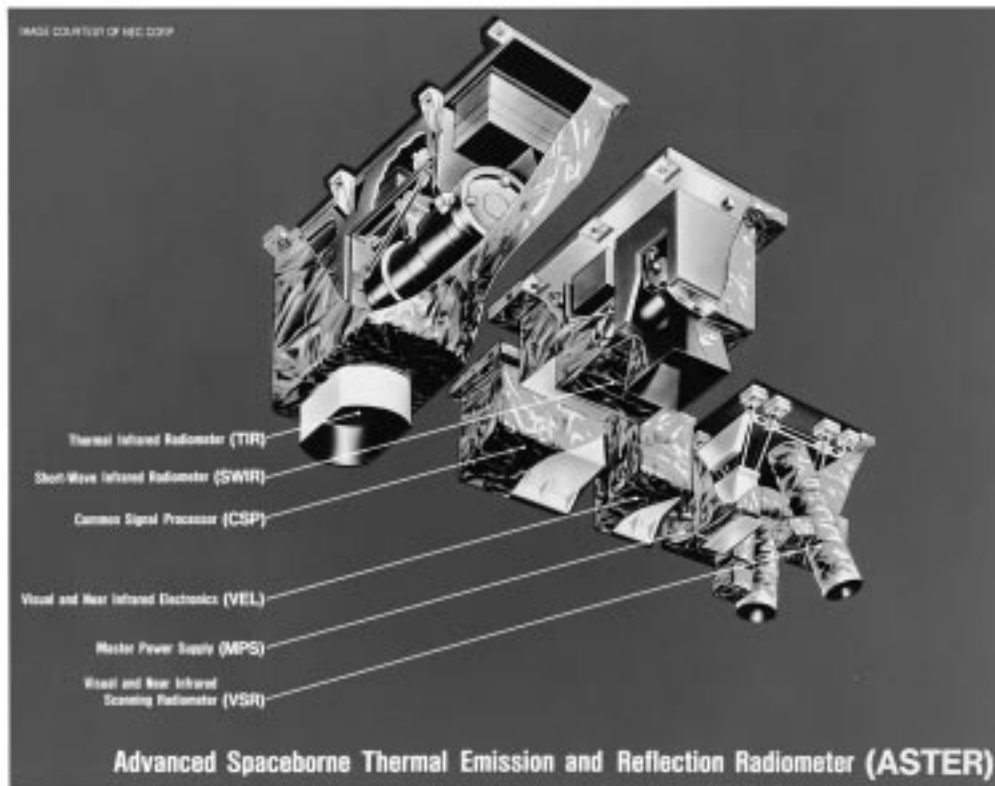


Fig. 1. Artist's view of the ASTER instrument.

spatial resolution. The VNIR bands will be useful in assessing vegetation and iron-oxide minerals in surface soils and rocks (Fig. 2).

The spectral bandpasses of the SWIR bands were selected mainly for the purpose of surface soil and mineral mapping. Band 4 is centered at the 1.65- μm region, and bands 5–9 target the characteristic absorption features of phyllosilicate and carbonate minerals in the 2.1–2.4 μm region. The ASTER SWIR will permit more detailed surface soil and lithologic

mapping than Landsat TM and JERS-1 OPS. Discrimination of clouds from snow will also be possible using the SWIR bands.

The ASTER TIR subsystem has five bands in the thermal infrared region, as shown in Fig. 3. Emissivity patterns derived from the five TIR bands will be used to estimate silica content [5]–[7], which is important in characterizing silicate rocks—the most abundant rock type on the earth's surface. The ASTER Science Team is currently developing algorithms

TABLE II
CHARACTERISTIC FUNCTIONS OF THE ASTER SUBSYSTEMS [11]

Item	VNIR	SWIR	TIR
Scan	Pushbroom	Pushbroom	Whiskbroom
Telescope optics	Refractive (Schmidt) D=82.25 mm (Nadir) D=94.28 mm (Backward)	Refractive D=190 mm	Reflective (Newtonian) D=240 mm
Spectrum separation	Dichroic and bandpass filter	Bandpass filter	Bandpass filter
Focal plane (Detector)	Si-CCD 5000 x 4	PtSi-CCD 2048 x 6	HgCdTe (PC) 10 x 5
Cryocooler	not cooled	Stirling cycle, 77 K	Stirling cycle, 80 K
Cross-track pointing	Telescope rotation ±24 degrees	Pointing mirror rotation ±8.55 degrees	Scan mirror rotation ±8.55 degrees
Thermal control	Radiation	Cold plate	Cold plate
Calibration	2 sets of Halogen lamps and monitor diodes	2 sets of Halogen lamps and monitor diodes	Blackbody 270 - 340 K

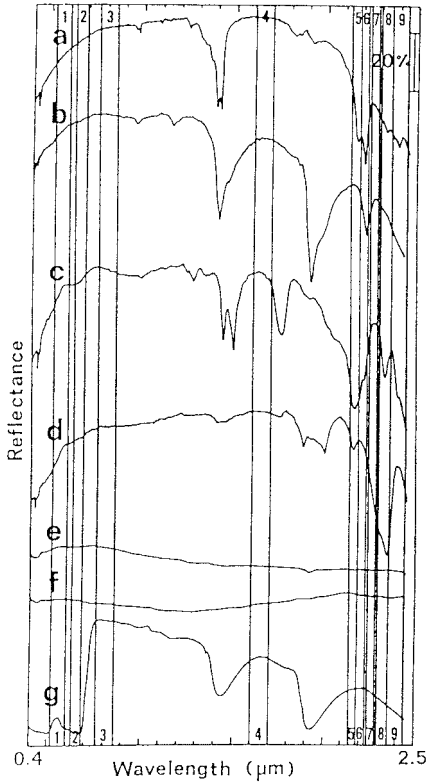


Fig. 2. Spectral bandpasses of the ASTER VNIR and SWIR, and the reflectance spectra of typical minerals, rocks, and vegetation: (a) kaolinite, (b) montmorillonite, (c) alunite, (d) calcite, (e) andesite, (f) granite, and (g) green leaves.

to separate temperature and emissivity of the surface materials [8]. Having multispectral TIR data allows for a more accurate determination of the variable spectral emissivity of the land surface and, hence, a more accurate determination of the land surface temperature.

Fig. 4 shows simulated ASTER images made from coregistered Airborne Visible/Infrared Imaging Spectrometer (AVIRIS) data (the VNIR and SWIR images) and Thermal Infrared Multispectral Scanner (TIMS [9]) data (the TIR image). The VNIR image (left) has a spatial resolution of 15 m and displays ASTER bands 3, 2, and 1 in red, green, and blue (RGB), respectively. The SWIR image (center) has a resolution of 30 m and combines SWIR bands 8, 6, and 4 as RGB, respectively. The TIR image (right) uses bands 14, 12, and 10 displayed as RGB, respectively, and has a resolution

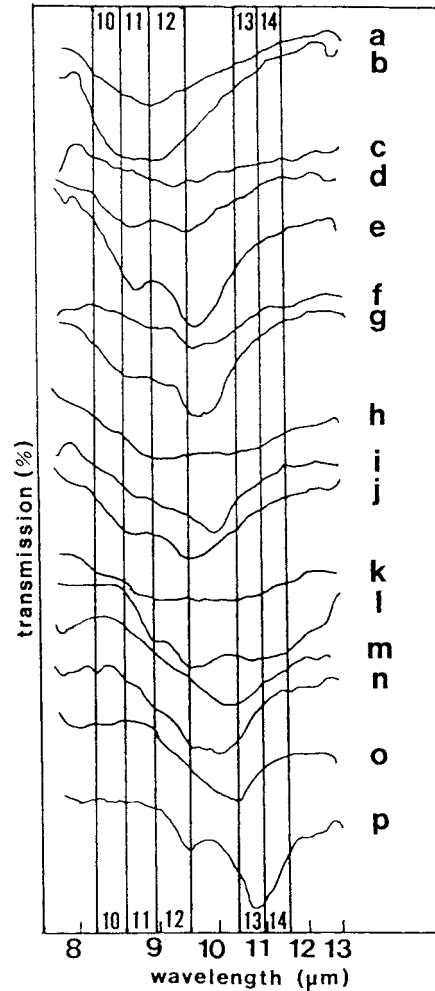


Fig. 3. Spectral bandpasses of the ASTER TIR, and the emissivity (transmission) spectra of typical rocks (modified from Vickers and Lyon, 1967): (a) dacite, (b) granite, (c) pumice, (d) trachyte, (e) quartz syenite, (f) andesite, (g) nephelene syenite, (h) hypersthene andesite, (i) quartz diorite, (j) augite diorite, (k) basalt, (l) plagioclase basalt, (m) peridotite, (n) serpentinite, (o) limburgite, and (p) dunite.

of 90 m. All of the composites have been enhanced using a decorrelation stretch algorithm. The size of the area depicted is 12 x 50 km.

Badwater, Death Valley, CA, is the lowest place in the United States. It is in the bottom middle of Fig. 4. The three versions of ASTER data illustrate the different compositional information available in various wavelength regions. For ex-

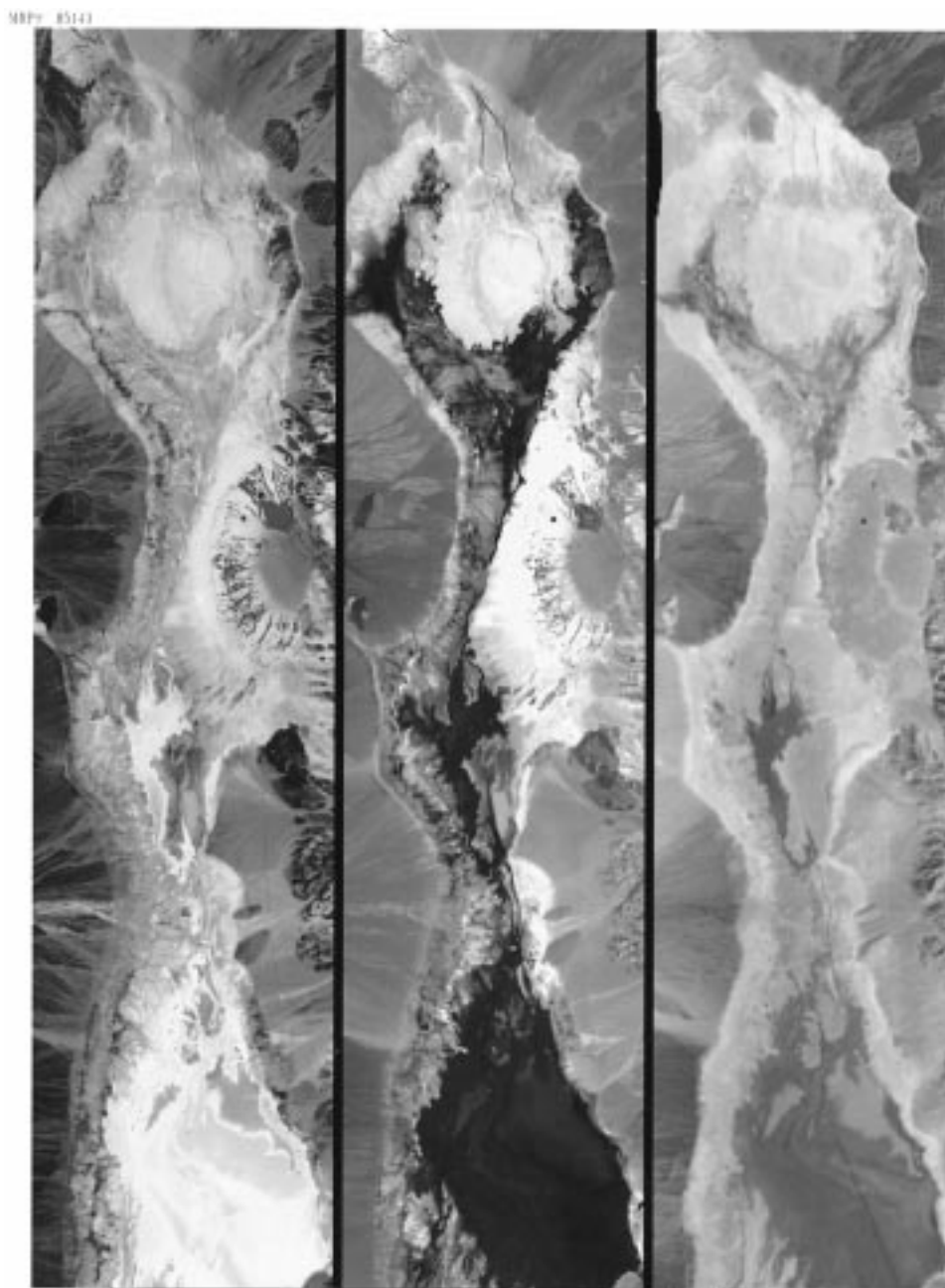


Fig. 4. Simulated ASTER images of Death Valley, CA; left: VNIR, center: SWIR, and right: TIR. The three versions of ASTER data illustrate the different compositional information available in various wavelength regions. For example, the bright red areas in the VNIR image are vegetation patches at Furnace Creek Ranch and on the Furnace Creek Fan. The turquoise area in the upper left corner of the SWIR image depicts ground covered by limestone fragments. In the TIR image, surfaces with the mineral quartz present are depicted in red.

ample, the bright red areas in the VNIR image are vegetation patches at Furnace Creek Ranch and on the Furnace Creek Fan. The turquoise area in the upper left corner of the SWIR image depicts ground covered by limestone fragments. In the TIR image, surfaces with the mineral quartz present are depicted in red.

C. Radiometric Performance

The requirements for the absolute radiometric accuracy of the VNIR and SWIR bands are specified to be better than $\pm 4\%$ at high-level input radiance. The absolute radiometric accuracy for the TIR bands is specified to be ± 3 K or less

at 200–240 K, ± 2 K or less at 240–270 K, ± 1 K or less at 270–340 K, and ± 9 K or less at 340–370 K.

The input energy, which defines the conditions specifying the radiometric resolution, is determined by the target radiance in front of each radiometer, and is called the input radiance. The maximum, high-level, and low-level radiances are specified as shown in Table III. The specification on radiometric accuracy is applied to the high-level radiance, unless otherwise specified.

The maximum input radiance, specified by a value 20% larger value than the high-level input radiance, is employed not only to avoid saturation for targets with very high reflectance,

TABLE III
INPUT RADIANCE [$W/(m^2 \text{ sr } \mu\text{m})$] FOR ASTER SPECTRAL BANDS

Subsystem	Band No.	Maximum Input Radiance	High Level Input Radiance	Low Level Input Radiance
VNIR	1	427	356	71.2
	2	358	298	59.6
	3N	218	182	36.4
	3B	218	182	36.4
SWIR	4	55.0	45.8	9.16
	5	17.6	14.7	2.94
	6	15.8	13.2	2.64
	7	15.1	12.6	2.52
	8	10.55	8.79	1.76
	9	8.04	6.70	1.34
TIR	10 - 14	Radiance of 370 K Blackbody	Radiance of 300 K Blackbody	Radiance of 200 K Blackbody

such as clouds, but also to compensate for possible errors in the model calculation. The concept of low-level input radiance, specified as 20% of the value of the high-level input radiance, is necessary for targets with low reflectance and for a large solar zenith angle. For the TIR bands, the input radiance is specified by blackbody temperature, since it is not only simple, but also convenient for the instrument performance tests, which use a blackbody as a source of radiation.

The VNIR and SWIR subsystems have three and four gains, respectively, as shown in Table IV. The gain setting for each band can be selected independently. The high gain setting is used to expand the range of output DN's for a low reflectance target. For instance, the high gain setting will be used for imaging vegetation and dark soil/rocks in the VNIR bands 1 and 2. The multiplication factors are specified as 2.5 for band 1 and 2.0 for the other VNIR and SWIR bands. The low gain setting is provided to accommodate an unexpectedly bright target, although almost all targets are expected to be observable at the normal gain. The low gain-2, available only for the SWIR bands, will be used for observation of high-temperature targets, such as a lava lake of an active volcano. Table V shows the highest temperature to be resolved by the SWIR bands. These values were calculated from the saturation levels of the charge coupled device (CCD) linear array.

The ASTER radiometric calibration plan is comprehensively described by Ono *et al.* [10]. In the preflight phase, the instrument, including imaging radiometers and the internal onboard calibration units, is calibrated against standard sources. It is likely that the instrument performance will change in orbit because of contamination and degradation of optical components, detectors, electronics, etc., during its six-year mission period. Therefore, internal onboard calibration units will be used for periodic calibrations of the radiometer in orbit. A two-point calibration is the basic approach in the reflected solar region (VNIR and SWIR) to determine the offset and the responsivity. The onboard calibration units for the VNIR and SWIR subsystems consist of a highly stable halogen lamp as a radiation source, optics to collect radiation from the lamp and direct it as a reference beam to the radiometer, and photodetectors to monitor the lamp radiation and/or the reference beam flux. Dual onboard calibration systems are used to enhance reliability in the VNIR and SWIR subsystems, respectively. The two identical onboard calibration units cross check the performance of each other periodically in orbit. If any change is detected between consecutive inflight calibra-

TABLE IV
GAIN SWITCHING FUNCTIONS (MULTIPLICATION FACTORS)

Subsystem	Band no.	High gain	Normal gain	Low gain -1	Low gain -2
VNIR	1	2.5	1.0	0.75	N/A
	2	2.0	1.0	0.75	N/A
	3N, 3B	2.0	1.0	0.75	N/A
SWIR	4	2.0	1.0	0.75	0.75
	5	2.0	1.0	0.75	0.17
	6	2.0	1.0	0.75	0.16
	7	2.0	1.0	0.75	0.18
	8	2.0	1.0	0.75	0.17
	9	2.0	1.0	0.75	0.12
TIR	10 - 14	N/A	N/A	N/A	N/A

TABLE V
SWIR SATURATION LEVELS AND THE HIGHEST OBSERVABLE TEMPERATURE

	Band 4	Band 5	Band 6	Band 7	Band 8	Band 9
Saturation radiance ($W/m^2/str/\mu\text{m}$)	73.3	103.5	98.7	83.8	62.0	67.0
Temperature (K)	739	658	649	631	603	599

tions, it is possible to infer and identify which component has changed: the ASTER radiometer, halogen lamp, calibration optics, or photodetectors. The radiometer's radiance data will be corrected for the identified change. The requirements on the absolute radiometric accuracy are not applicable to the VNIR backward-viewing band, as the major purpose of this band is stereoscopic observation with the nadir viewing band 3. For this reason, the backward-viewing band does not have an onboard calibration lamp.

For the TIR subsystem, two-point calibration is also desirable, for instance, an onboard blackbody radiator at the environmental temperature for a high-level input and cold space for a low-level input. However, the present ASTER instrument design does not allow the TIR radiometer to view cold space due to mechanical and spacecraft interface reasons. Thus, it was decided to vary the temperature of the onboard blackbody radiator over about 70 K, from about 270 to 340 K. The TIR temperature scale is interpolated within and extrapolated outside the variable temperature range. The emissivity and radiative environments are well characterized to evaluate the emissive component as well as the reflective component. Emissivity change due to contamination and degradation in orbit will be estimated.

In addition to the onboard calibrators, reflectance-, radiance-, and emittance-based methods of vicarious calibration using measured ground and lunar reference sites will also be employed. Calibration coefficients will be calculated by averaging with weighted coefficients the calibration data from the various methods. The coefficients will be updated periodically.

D. Geometric Performance

Spatial resolution of the ASTER subsystems is 15 m for VNIR, 30 m for SWIR, and 90 m for TIR. While the spatial resolution of the SWIR and TIR are lower than that of the VNIR, they are still the highest among all of the EOS-AM1 instruments in their wavelength regions. The ASTER data are expected to provide substantial information for subpixel scale analysis of the other instruments' data, e.g., MODIS with 250-

500-, or 1000-m spatial resolution and MISR with 275-, 550-, or 1100-m resolution.

The band-to-band registration (BBR) requirements from the ASTER Science Team are ± 0.2 pixels in the same telescope and 0.3 pixels (of the coarser spatial resolution) among the different telescopes after necessary ground processing. The details of protoflight model (PFM) tests are reported elsewhere in this issue by Fujisada *et al.* [11]. The BBR of intertelescopes and intratelescopes will be carried out in the Level 1 data processing [12].

After launch, the registration will be verified by cross correlation between images containing many well-defined, high-contrast features.

E. Stereo Capability

The VNIR subsystem has one backward-viewing band for stereoscopic observation in the along-track direction. The nadir-backward stereo-viewing geometry of the VNIR gives a higher probability of obtaining a cloud-free image pair, as compared to a side stereo observation system requiring multiorbit observations, such as the SPOT HRV. The base-height (BH) ratio is 0.6. Digital elevation models (DEM) can be generated from stereo data. The height accuracy of the DEM depends upon the BH ratio, spatial resolution, and error in the parallax measurement. The ASTER DEM height accuracy should be 7–50 m, and the scale of topographic maps to be generated from the ASTER stereo data will be 1:50 000–1:200 000, if we assume 0.5–1.0 pixel, respectively, as the total parallax error. The ability to control the parallax error depends on the availability and accuracy of ground control points. More details are discussed by Welch *et al.* [13].

F. Pointing Capability

All ASTER bands will cover the same 60-km imaging swath with a pointing capability in the cross-track direction to cover ± 116 km from the nadir, so that any point on the globe is accessible at least once every 16 days with the full spectral coverage provided by the VNIR, SWIR, and TIR. Three pointing positions (nadir, left, and right) are necessary to cover the earth's surface at the equator, where the EOS-AM1 orbit separation is 172 km. The use of an additional four intermediate pointing positions, which are located right on the boundaries of the swaths of the three nominal pointings, will allow us to obtain small targets within a single scene, if the target is smaller than 60 km in diameter and located on the boundary of two of the three nominal swaths.

It is expected that most of the emergency targets can be covered with these seven pointing positions, although the option remains open to use any intermediate pointing position in rare, special cases. The VNIR subsystem has a larger pointing capability, up to 24° , and thus, the swath center is pointable up to ± 318 km from the nadir. This capability was added to shorten the potential delay period for a time-critical observation of natural hazards, like volcanic eruptions and floods. The recurrent pattern for a target on the equator using 24° pointing becomes 2-5-2-7 days (four days average).

TABLE VI
ASTER OPERATION MODES

Operation modes		Subsystem			Data rates
		VNIR	SWIR	TIR	
Daytime	Full mode	O	O	O	89.2 Mbps
	VNIR mode	O			62.038 Mbps
	Stereo mode	O			31.019 Mbps
	TIR mode			O	4.109 Mbps
Nighttime	TIR mode			O	4.109 Mbps
	Volcano mode		O	O	27.162 Mbps

III. OPERATION SCENARIO

A. Operation Constraints

There are several constraints on ASTER data acquisition. Limitations on data acquisition derive from a variety of sources, including limits on the number of telescope pointing changes during mission, dissipation of heat, volume of data that can be stored in the EOS-AM1 solid-state recorder, available power for ASTER, bandwidth of downlink, length of each downlink window, frequency of downlink windows, and finally, the ability to schedule ASTER instrument activities.

The primary limitations on ASTER data collection are the data volume allocated to the instrument in EOS-AM1's memory (solid-state recorder) and in the communications link with the Tracking and Data Relay Satellite System (TDRSS) and ground stations. The maximum average data rate allocated to ASTER, based on a two-orbit average, is 8.3 Mbps, which roughly corresponds to 8 min of full-mode daytime operation plus 8 min of nighttime TIR operation per orbit. The single orbit maximum data acquisition time is 16 min, if no data is acquired in both previous and following orbits. The peak data rate and peak power consumption are 89.2 Mbps and 726 W, respectively. Given that the instrument is scheduled to operate for six years, ASTER could collect approximately 1.7 million scenes of full-mode data. In practice, there will be factors that will decrease this amount, such as scheduling inefficiencies.

B. Operation Modes

The three ASTER subsystems can be operated independently. In addition, there are several possible instrument gain settings and pointing angles. This results in many possible observation modes. However, several nominal modes have been defined. The nominal daytime mode is simultaneous data acquisition using the three subsystems looking at the same 60-km imaging swath. The nominal nighttime mode is TIR-only operation. Flexibility in operations has been requested from the ASTER Science Team to obtain as much data as possible while keeping within the allocated data rate. Therefore, as shown in Table VI, four additional nominal modes have been defined.

The daytime VNIR mode will be used for areas where high-resolution VNIR data are essential, but SWIR and TIR spectral data are not necessary. In the daytime stereo mode, only the bands 3N (nadir) and 3B (backward) will be operated for the purpose of stereo imaging. If a pointing angle of greater than 8.55° is needed, the daytime VNIR or stereo mode can be used, pointing out to $\pm 24^\circ$. The TIR mode is also available in daytime. The open ocean will usually be observed in TIR

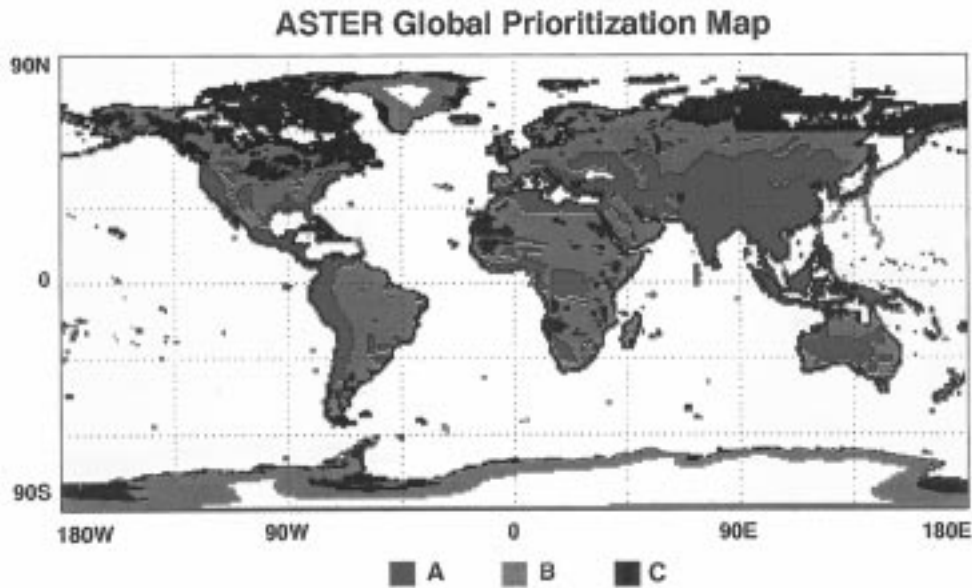


Fig. 5. Various regions of the earth have been assigned different priorities for acquiring ASTER Global Map data; A: high, B: medium, and C: low.

mode since most ocean surface targets will not have interesting signatures in ASTER's VNIR or SWIR bands. These three modes (daytime VNIR, daytime stereo, and daytime TIR) are complementary to the daytime full mode and will be used only when allocated resources cannot permit the full mode. For instance, periodic monitoring of the Antarctic glacier boundaries is one objective of the ASTER Science Team that can be accomplished using the daytime stereo mode.

The earth's nighttime hemisphere will usually be observed only in TIR mode. However, it will be possible to use the SWIR bands at night. Such an occasion might arise if a target temperature is higher than the maximum input radiance for the TIR bands, which could occur with high-temperature targets, like wildfires, lava lakes, or active volcano flows. The SWIR bands can measure surface temperatures up to about 650 K, with 30-m ground resolution in nighttime, as shown in Table V. Moreover, the time necessary to observe hot targets can be shortened by combining the daytime full mode and nighttime volcano mode.

C. Data Collection Categories

ASTER data types consist of 1) engineering data that are required to monitor and maintain spacecraft and instrument health and safety, 2) calibration data that are obtained as a part of both onboard and vicarious calibration of the instrument, and 3) science data that are collected to meet the science objectives of the mission. Furthermore, to better manage the allocation of ASTER observing resources, three data collection categories for the science data have been defined. These categories are based on data set size and science objectives. They are listed below.

1) *Global Mapping*: The global data set will be used by investigators of every discipline to support their research. The high spatial resolution of the ASTER Global Map will complement the lower resolution data acquired more frequently by other EOS instruments, such as MODIS and MISR. The

ASTER global data set will include images of the entire earth's land surface using all ASTER spectral bands and stereo. This global data set will be composed of those images that best meet the Global Map quality criteria and identified in the mission image database. Each ASTER observation (regardless of whether it was originally scheduled for a local observation, regional monitoring, or the global map) will be assessed by the Science Team for its probability of significantly increasing the quality of the global data set. Currently the following characteristics have been identified for images in the Global Map data set:

- 1) one-time coverage;
- 2) high sun angle;
- 3) optimum gain for the local land surface;
- 4) minimum snow and ice cover;
- 5) minimum vegetation cover; and
- 6) no more than 20% cloud cover (perhaps more for special subregions).

As shown in Fig. 5, the land surface of the earth has been prioritized by the ASTER Science Team for observation as part of the Global Map. This prioritization is reflected in the prioritization algorithm to be used in the ASTER scheduler.

2) *Regional Monitoring*: Regional data sets contain the data necessary for analysis of a large region or a region requiring multitemporal analysis. One example might be imaging the advance and retreat of all mountain glaciers in the Himalayas as a function of season for the six-year life of the mission. Another example might be analyzing changes in forest cover and resulting changes in air-surface moisture fluxes for the state of Rondonia (in the Brazilian Amazon) over six years. Some regional data sets may require only single-time images of a large region.

3) *Local Observations*: Local observations will be made in response to Data Acquisition Requests (DAR's) from individual investigators or investigation teams. Approved EOS investigators are authorized to submit requests for new ASTER

data acquisition. Other investigators can apply for such authorization to either NASA or MITI. Anyone can request existing data. Local observations might include, for example, scenes for analyzing land use, surface energy balance, or local geologic features. A subset of local observations are images of such ephemeral events as volcanoes, floods, or fires. Requests for “urgent observations” of such phenomena must be fulfilled in short-time periods (of a few days). These requests receive special handling.

A “local observation” data set and a “regional monitoring” data set are distinguished by the amount of viewing resources required to satisfy the request. Smaller requirements are defined as local observations, and larger requirements are defined as regional monitoring. The cutoff between the two will be set by the Science Team and subject to change as the mission proceeds.

There are several types of instrument activity requests, collectively termed “xAR’s.” Approved ASTER investigators can request activities relating to data acquisitions via DAR’s. Local observations are made in response to DAR’s from individual investigators or individual teams. In cases where the request results in a major load on the instrument resources or where the request can be used to satisfy a large number of users, the request will be from the Science Team in the form of Science Team Acquisition Requests (STAR’s). There are three types of STAR’s; STAR-local, STAR-regional, and STAR-global mapping. Examples of the STAR-local include observation requests for vicarious calibration, algorithm validation, etc. Another type of xAR is the Engineering Team Requests (ETR), which is used by the instrument engineering team to request instrument activities for the purpose of instrument calibration, health, and safety.

D. Prioritization and Scheduling

The ASTER scheduler will choose between different observation alternatives for each small increment of time (from 1 to 4.5 s) in the schedule being generated, in a manner designed to maximize the science return over a time period of a day. The scheduling algorithm uses a prioritization function to rank the alternative observing modes (and other operating modes) for each time-step. The output schedule can be modified by changing the scheduler’s input parameters; the ASTER Science Team and the Science Scheduling Support Group (SSSG) are responsible for choosing these input parameters.

Although ASTER could collect as many as 1.7 million scenes of full-mode data during the mission, there will be factors that will decrease this amount, such as scheduling inefficiencies. The purpose of the scheduling process and the scheduler software is to maximize the scientific content of each scene.

The scheduler will be able to generate an ASTER activity schedule of any length by specifying the start and end times of a schedule as input parameters. For any length schedule, the scheduler will determine ASTER activities one day at a time.

Prioritization is the process of ranking possible observations, so that the observation opportunities with higher scientific or programmatic value are given higher probabilities of be-

TABLE VII
ASTER STANDARD (1A TO 4A21) AND
SEMISTANDARD (3A01 AND 4A01) DATA PRODUCTS

Product code	Product name	Japan	US
1A	Reconstructed, unprocessed instrument data	O	—
2B	Radiance at sensor	O	—
2A01	Brightness temperature at sensor	X	O
2A02	Relative spectral emissivity (D-stretch)	O	O
2A03	Relative spectral reflectance (D-stretch)	O	O
2B01	Surface radiance	O	O
2B03	Surface temperature	O	O
2B04	Surface emissivity	O	O
2B05	Surface reflectance	O	O
4A	Polar cloud map (after launch)	X	O
4A21	Digital elevation model (absolute)	X	O
3A01	Radiance at sensor with ortho-photo correction	O	—
4A01	Digital elevation model (relative)	O	—

ing scheduled. The scheduler uses the prioritization function to calculate a priority for each potential observation. The weighting factors in this function are determined by the Science Team and may be modified as the mission progresses. The prioritization function uses information from all xAR’s requesting a possible observation, along with some time-dependent and instrument information, as input variables.

The scheduler must select between a variety of instrument configurations, each of which is a unique combination of observing mode, telescope gain settings, and cross-track viewing angle. For each 1–4.5-s time-step, the scheduler calculates the priority of observations in each instrument configuration. A time sequence of priorities, for a single instrument configuration, is called a “priority curve.” After calculating all of the priority curves, the scheduler searches among all curves for the instrument configuration that have the maximum priority for any time-step in the entire day. The instrument is then scheduled to observe in that instrument configuration during that time-step. The scheduler then searches for the next highest priority instrument configuration, which is then scheduled for that configuration’s time-step. This continues until all time-steps in the entire day have been scheduled. At each point in this process, the scheduler checks to make sure that no operating constraints are being violated.

IV. DATA PRODUCTS

Table VII shows a list of data products that will be provided by the ASTER Science Team. The Japanese are responsible for providing ASTER Level 1 data products. The details of the algorithm to generate the ASTER Level 1 data products are described in Fujisada *et al.* [12]. The standard Level 2 data products will be produced in both the United States and Japan. All algorithms used in both Japan and the United States are identical in principle, although the source codes and executable programs may be different due to different machine and software environments. Algorithm development has been carried out collaboratively by Japan and the United States. Standard data products will be provided to users on a nondiscriminatory basis from the United States Earth Observing System Data and Information System (EOSDIS) and the Japanese ASTER GDS. The latter is described by Watanabe *et al.* [14]. Any user can submit a Data Product Request (DPR) to obtain a standard data product. Production

of a standard data product is guaranteed, if all necessary inputs (e.g., cloud-free Level 1 data, input for atmospheric correction, etc.) to generate the data product are available. Development and validation of standard data products for ASTER will continue throughout the mission. Some new products may include a variety of vegetation and cloud parameters.

The category of semistandard data products is defined only for the Japanese ASTER GDS. A user can submit a DPR; however, production of a semistandard product is not guaranteed, as the production schedule will be controlled not only by DPR's, but also by a long-term plan to be prepared by the ASTER Science Team. There are also several special data products proposed by the ASTER Science Team members; e.g., soil maps, mineral and rock maps, volcano maps, wetland maps, coral reef maps, vegetation index, aquatic plant distribution, turbidity, etc. These will be produced at the Science Team Member facilities on a research basis.

V. RESEARCH PLANS

ASTER data will be useful to study various local to regional phenomena. Some specific areas of science have been identified as the following:

- 1) land surface climatology—investigation of land surface parameters, surface temperature, etc., to understand land-atmosphere interaction and energy and moisture fluxes (evaporation and evapotranspiration);
- 2) vegetation and ecosystem dynamics—investigations of vegetation and soil distribution and their changes to estimate biological productivity, understand land-atmosphere interaction, and detect ecosystem changes;
- 3) volcano monitoring—monitoring of eruptions and precursive events, such as emission of volcanic gases to the atmosphere, eruption plumes, development of lava lakes and fumarolic activity, eruptive history and eruptive potential;
- 4) hazard monitoring—observation of the extent and effects of wildfires, flooding, landslides, and coastal erosion;
- 5) aerosols and clouds—observation of atmospheric aerosol characteristics and various cloud types, which are useful for the atmospheric correction of surface retrievals;
- 6) carbon cycling in the marine ecosystem—determination of the atmospheric carbon dioxide being fixed into coral reefs by measuring the global distribution and accumulation rate of coral reefs;
- 7) hydrology—understanding global energy and hydrologic processes and their relationship to global changes;
- 8) geology, and soil—the detailed compositional and geomorphologic mapping of surface soil and bedrocks to study the land surface processes and the earth's history; and
- 9) land surface and land cover change—monitoring of desertification, deforestation, urbanization, etc.

A few examples of research topics currently being pursued by the EOS Interdisciplinary Science Principal Investigators (IDS PI's) and the ASTER Science Team (AST) members include the following:

- 1) global assessment of active volcanism, volcanic hazards, and volcanic inputs to the atmosphere from EOS (EOS IDS PI—Mouginis-Mark; AST—Urai, Fukui, Pieri, and Kahle);
- 2) hydrology, hydrochemical modeling, and remote sensing in snow-covered Alpine drainage basins (EOS IDS PI—Dozier);
- 3) climate, erosion, and tectonics in mountain systems (EOS IDS PI—Isacks);
- 4) hydrologic cycle and climatic process and semiarid lands (EOS IDS PI—Kerr);
- 5) lithologic mapping in arid regions (AST—Yamaguchi and Tsuchida);
- 6) spatial variation of surface energy and mass fluxes over land surfaces at microscales and mesoscales (AST—Schieldge);
- 7) estimation of SiO₂ content of igneous rocks using ASTER TIR data (AST—Ninomiya);
- 8) mapping and monitoring of coral reefs (AST—Matsunaga and Kayane);
- 9) mapping carbonatite and alkaline rocks in African Rift Valley (AST—Rowan);
- 10) paleoclimatology based upon glacial monitoring in Central Asia (AST—Gillespie);
- 11) monitoring the glaciers of Antarctic coastal regions (AST—Kieffer).

ACKNOWLEDGMENT

The authors wish to thank the ASTER Science Team members for their helpful discussions.

Reference herein to any specific commercial product, process, or service by trade name, trademark, manufacturer or otherwise, does not constitute or imply endorsement by NASA, the United States Government, or Jet Propulsion Laboratory, California Institute of Technology.

REFERENCES

- [1] Y. Yamaguchi, H. Tsu, and H. Fujisada, "Scientific basis of ASTER instrument design," in *Proc. SPIE*, 1993, vol. 1939, pp. 150–160.
- [2] Y. Yamaguchi, H. Tsu, H. Fujisada, A. B. Kahle, and D. A. Nichols, "ASTER instrument design and science objectives," *Amer. Inst. Aeron. Astron.*, vol. 7, paper 94-0597, 1994.
- [3] A. B. Kahle, F. Palluconi, S. Hook, V. J. Realmuto, and G. Bothwell, "The Advanced Spaceborne Thermal Emission and Reflectance Radiometer (ASTER)," *Int. J. Imaging Syst. Tech.*, vol. 3, pp. 144–156, 1991.
- [4] H. Fujisada, "Overview of ASTER instrument on EOS AM-1 platform," in *Proc. SPIE*, 1994, vol. 2268, pp. 14–36.
- [5] R. S. Vickers and R. J. P. Lyon, "Infrared sensing from spacecraft—A geologic interpretation," in *Proc. Thermophysics Special Conf.*, *Amer. Inst. Astron.*, paper 67-284, 1967.
- [6] G. R. Hunt, "Electromagnetic radiation: The communication link in remote sensing," in *Remote Sensing in Geology*, G. S. Siegel and A. R. Gillespie, Eds. New York: Wiley, 1980, pp. 5–45.
- [7] Y. Ninomiya, "Quantitative estimation of SiO₂ content in igneous rocks using thermal infrared spectra with a neural network approach," *IEEE Trans. Geosci. Remote Sensing*, vol. 33, pp. 684–691, May 1995.
- [8] A. Gillespie, S. Rokugawa, T. Matsunaga, J. S. Cothorn, S. Hook, and A. B. Kahle, "A temperature and emissivity separation algorithm for Advanced Spaceborne Thermal Emission and Reflection Radiometer (ASTER) images," this issue, pp. 1113–1126.
- [9] A. B. Kahle and A. F. H. Goetz, "Mineralogic information from a new airborne thermal infrared multispectral scanner," *Science*, vol. 222, no. 4619, pp. 24–27, 1983.

- [10] A. Ono, F. Sakuma, K. Arai, Y. Yamaguchi, H. Fujisada, P. N. Slater, K. Thome, F. Palluconi, and H. H. Kieffer, "Pre-flight and inflight calibration plan for ASTER," *J. Atmos. Ocean. Technol.*, vol. 13, no. 2, pp. 321–335, 1996.
- [11] H. Fujisada, F. Sakuma, A. Ono, and M. Kudoh, "Design and preflight performance of ASTER instrument protoflight model," this issue, pp. 1152–1160.
- [12] H. Fujisada, "ASTER Level-1 data processing algorithm," this issue, pp. 1101–1112.
- [13] R. Welch, T. Jordan, H. Lang, and H. Murakami, "ASTER as a source for topographic data in the late 1990's," this issue, pp. 1282–1289.
- [14] H. Watanabe, H. Fujisada, and I. Sato, "Preliminary design concept of ASTER ground data system," in *Proc. SPIE*, 1995, vol. 2583, pp. 26–40.
- Hiroji Tsu**, photograph and biography not available at the time of publication.
- Toru Kawakami**, photograph and biography not available at the time of publication.
- Moshe Pniel**, photograph and biography not available at the time of publication.

Yasushi Yamaguchi, for a photograph and biography, see p. 731 of the May 1998 issue of this TRANSACTIONS.

Anne B. Kahle, photograph and biography not available at the time of publication.